Molecular Vibration Analysis of the $TeCl_4$ Tetramer and Monomer and the $SeCl_4$ Tetramer

S. J. Cyvin and B. N. Cyvin
Institutt for teoretisk kjemi, Universitetet i Trondheim *

W. Brockner and A. F. Demiray
Anorganisch-Chemisches Institut, Technische Universität Clausthal **

Z. Naturforsch. **33**c, 714–721 (1978); received March 6, 1978

The molecular vibrations of $(TeCl_4)_4$ and $(SeCl_4)_4$ are studied on the basis of a cubane-like T_d model. Symmetry coordinates are produced by using the theory developed for tetrahedral complexes with trigonal ligands. Approximate vibrational frequencies are calculated from very simple four-parameter force fields and used as an aid in tentative assignments of observed frequencies from literature. Next the force fields are refined by adjustments to the observed frequencies assigned as fundamentals. Potential energy distribution terms and mean amplitudes of vibration are calculated. Finally the monomeric form of $TeCl_4$ is analysed, mainly in order to show the frequency shifts on passing from the monomer to tetramer.

Introduction

The tetrahalides of group VI elements have interesting structural properties. In the gas phase SF_4 has been investigated most extensively, both by electron diffraction [1, 2] and vibrational analysis [3–10]. The structure is known to be of C_{2v} symmetry, where two pairs of nonequivalent S–F are distinguished and referred to as axial and equatorial, respectively. This structure can also be described as trigonal bipyramidal with lone-pair electrons on one of its equatorial orbitals. The analogous structure was also reported for $TeCl_4$ in an early gas electron diffraction investigation [11] and similarly for SeF_4 [12]. An excellent X-ray work on the crystal structure of $TeCl_4$ has appeared [13, 14]. It is concluded that this compound exists as tetramers, $(TeCl_4)_4$ in the solid state and can be described as a cubane-like structure with four $TeCl_3^+$ ions linked together through four bridging Cl^- ions. Thus each Te atom is surrounded by three terminal (Cl_t) and three bridging (Cl_b) chlorine atoms in the staggered position. The whole $(TeCl_4)_4$ model has T_d symmetry in an idealized form where average distances are used for the Te–Cl_t bonds and the Te-Cl_b bridges. Structures isomorphous with $TeCl_4$ have been determined for $SeCl_4$ and $TeBr_4$ in the solid state [15, 16]. A recent nuclear quadrupole resonance investigation of $TeCl_4$ and $TeBr_4$ [17] has confirmed these findings. This paper refers to infrared experimental works of solid $TeCl_4$ and $TeBr_4$. Raman works on $TeCl_4$ and $SeCl_4$ are also available [18, 19] along with another significant work combining Raman and infrared spectra [20]. The bibliographies of the cited references may be consulted for numerous additional works in this area.

In spite of the numerous experimental works in vibrational spectroscopy for $TeCl_4$ and $SeCl_4$ in the solid state we have not found any report on a complete normal coordinate analysis for the tetrameric model of these compounds. In the present work this analysis bas been performed for the complete twenty-atomic model on the basis of the idealized tetrahedral (T_d) structure. The four $TeCl_3^+$ groups in $(TeCl_4)_4$ can be regarded as trigonal (C_{3v}) ligands in a tetrahedral complex. Hence the theory for constructing symmetry coordinates of molecular vibrations for such complexes [21–23] can be employed. This theory has previously been applied to $[Zn(NH_3)_4]^{2+}$ [24], $Pt(PF_3)_4$, $Pd(PF_3)_4$ and $Ni(PF_3)_4$ [25] and a $[PMo_{12}O_{40}]^{3-}$ model with the Keggin structure [26].

Valence Coordinates

Figure 1 shows the twenty-atomic molecular model with the adopted numbering of atoms. The M–Cl_b and M–Cl_t stretchings, where M = Te or Se, are identified by the symbols r and d, respectively. The identification system for the d coordinates, viz. (d_1^X, d_2^X, d_3^X), where X = A, B, C and D designates the ligand groups, is fully explained on Figure 2.

---

* Reprint requests to Prof. S. J. Cyvin, Division of Physical Chemistry, The University of Trondheim, N-7034 Trondheim-NTH, Norwegen.

** D-3392 Clausthal-Zellerfeld, Germany.

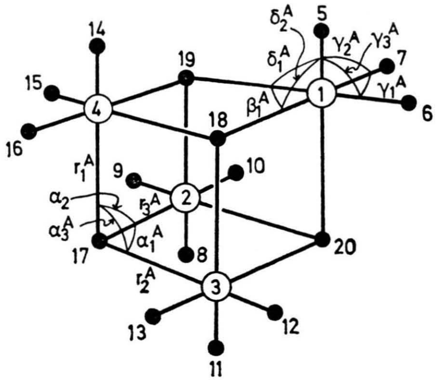

Fig. 1. The $(MCl_4)_4$ model; symmetry T_d. Some representative valence coordinates are indicated; see the text for full descriptions.

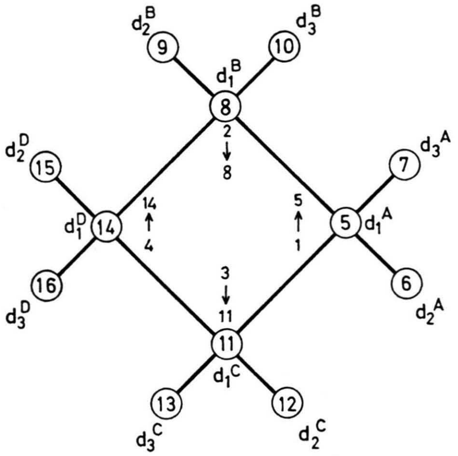

Fig. 2. The $(MCl_4)_4$ model with the $M\text{-}Cl_t$ stretching (d) coordinates. It is indicated that atom number 1 lies below atom 5, etc. Thus d_1^A, for instance, designates the 1—5 stretching.

The $(\gamma_1^X, \gamma_2^X, \gamma_3^X)$ Cl_tMCl_t bendings are defined as opposite to the (d_1^X, d_2^X, d_3^X) stretchings, respectively; cf. Figure 1. The (r_1^X, r_2^X, r_3^X) stretchings are chosen parallel to the (d_1^X, d_2^X, d_3^X) stretchings as exemplified for $X = A$ on Figure 1. Also the definition of the notation for the $(\alpha_1^X, \alpha_2^X, \alpha_3^X)$ MCl_bM bendings is explained on Fig. 1 using $X = A$ as the representative example. The Cl_bMCl_b bendings are designated β; they are exemplified by β_1^A on Figure 1. Finally we define twenty-four Cl_tMCl_b bendings (δ), six around each M atom, $(\delta_1^X, \ldots, \delta_6^X)$. For $X = A$ these six bendings involve the atoms 5-1-19, 5-1-18, 6-1-18, 6-1-20, 7-1-20 and 7-1-19, respectively.

Each bending, say $\varphi(i-k-j)$, was scaled by a factor with the dimension of length in the usual way: $(R_{ik} R_{jk})^{1/2} \varphi$.

Symmetry Coordinates

The normal modes of the whole model are distributed among the species of the T_d group according to

$$\Gamma(\text{total}) = 4A_1 + A_2 + 5E + 5F_1 + 8F_2 .$$

These modes may be classified as those of (a) $TeCl_3^+$ ligand vibrations, (b) vibrations of the Te_4Cl_4 cube, which arbitrarily may be referred to as „framework" [22] or „inter-ligand" [26] vibrations, and finally (c) couplings. The respective symmetric structures are:

$$\Gamma(a) = 2A_1 + 2E + 2F_1 + 4F_2 ,$$
$$\Gamma(b) = 2A_1 + 2E + F_1 + 3F_2 ,$$
$$\Gamma(c) = A_2 + E + 2F_1 + F_2 .$$

The different types of vibrations are represented by the types of valence coordinates in the following way:

(a) Ligand vibrations are described by the d and γ types.
(b) The cube vibrations are described by r and α.
(c) The couplings are described by τ. Here the τ coordinates are defined as normalized differences of scaled δ-type coordinates according to:

$$(\delta_1^X - \delta_2^X, \delta_3^X - \delta_4^X, \delta_5^X - \delta_6^X)$$

for $(\tau_1^X, \tau_2^X, \tau_3^X)$, respectively.

The valence coordinates specified under (a), (b) and (c) above are sufficient to construct a complete set of independent symmetry coordinates for the molecular vibrations. Thus all the β-type bendings and combinations with sums (rather than differences) of δ's are here taken as redundant coordinates. In addition there exist six redundant combinations of the α's in the present system.

The notation of valence coordinates is chosen here so as to make full advantage of the theory of constructing symmetry coordinates for tetrahedral complexes with trigonal ligands [21, 23]. Table 1 shows the types of coordinates used to construct the different symmetry coordinates within the T_d symmetry species. Each of these coordinates is constructed from intermediate combinations of the valence coordinates according to the trigonal (C_{3v})

Table 1. Types of symmetry coordinates for the $(MCl_4)_4$ model.

Species of T_d	No.	Type (Species of C_{3v})
A_1	1	$d(a_1)$
	2	$\gamma(a_1)$
	3	$r(a_1)$
	4	$\alpha(a_1)$
A_2	1	$\tau(a_2)$
E_1	1	$d(e)$
	2	$\gamma(e)$
	3	$r(e)$
	4	$\alpha(e)$
	5	$\tau(e)$
F_1	1	$d(e)$
	2	$\gamma(e)$
	3	$r(e)$
	4	$\tau(a_2)$
	5	$\tau(e)$
F_2	1	$d(a_1)$
	2	$\gamma(a_1)$
	3	$d(e)$
	4	$\gamma(e)$
	5	$r(a_1)$
	6	$\alpha(a_1)$
	7	$r(e)$
	8	$\tau(e)$

symmetry as indicated by the parenthesized symbols of the C_{3v} species. These intermediate combinations are:

For the ligand (a) and cube (b) vibrations

$$(a_1) \quad 3^{-1/2}(q_1{}^X + q_2{}^X + q_3{}^X)\,,$$
$$(e;\,a) \quad 6^{-1/2}(2q_1{}^X - q_2{}^X - q_3{}^X)\,,$$
$$(e;\,b) \quad 2^{-1/2}(q_2{}^X - q_3{}^X)\,,$$

where the q's represent any valence coordinate type except τ.

For the couplings (c)

$$(a_2) \quad 3^{-1/2}(\tau_1{}^X + \tau_2{}^X + \tau_3{}^X)\,,$$
$$(e;\,a) \quad 2^{-1/2}(-\tau_2{}^X + \tau_3{}^X)\,,$$
$$(e;\,b) \quad 6^{-1/2}(2\tau_1{}^X - \tau_2{}^X - \tau_3{}^X)\,.$$

As a result of the correlation schemes between the C_{3v} and T_d symmetry-adapted coordinate combinations we have deduced the coefficients of the final symmetry coordinates as shown in Table 2 for the ligand and cube vibrations and Table 3 for

Table 2. Coefficients of symmetry coordinates for ligand and cube vibrations in the $(MCl_4)_4$ model.

Species of T_d	(Species of C_{3v})	Norm. factor	Coefficients of											
			$q_1{}^A$	$q_2{}^A$	$q_3{}^A$	$q_1{}^B$	$q_2{}^B$	$q_3{}^B$	$q_1{}^C$	$q_2{}^C$	$q_3{}^C$	$q_1{}^D$	$q_2{}^D$	$q_3{}^D$
A_1	(a_1)	$12^{-1/2}$	1	1	1	1	1	1	1	1	1	1	1	1
$E;\,a$	(e)	$24^{-1/2}$	2	−1	−1	2	−1	−1	2	−1	−1	2	−1	−1
$E;\,b$	(e)	$8^{-1/2}$	0	1	−1	0	1	−1	0	1	−1	0	1	−1
$F_1;\,a$	(e)	1/4	2	−1	−1	0	−1	1	0	1	−1	−2	1	1
$F_1;\,b$	(e)	1/4	0	1	−1	−2	1	1	2	−1	−1	0	−1	1
$F_1;\,c$	(e)	$8^{-1/2}$	0	1	−1	0	−1	1	0	−1	1	0	1	−1
$F_2;\,a$	(a_1)	$6^{-1/2}$	1	1	1	0	0	0	0	0	0	−1	−1	−1
$F_2;\,b$	(a_1)	$6^{-1/2}$	0	0	0	1	1	1	−1	−1	−1	0	0	0
$F_2;\,c$	(a_1)	$12^{-1/2}$	1	1	1	−1	−1	−1	−1	−1	−1	1	1	1
$F_2;\,a$	(e)	$48^{-1/2}$	2	−1	−1	0	3	−3	0	−3	3	−2	1	1
$F_2;\,b$	(e)	$48^{-1/2}$	0	3	−3	2	−1	−1	−2	1	1	0	−3	3
$F_2;\,c$	(e)	$24^{-1/2}$	−2	1	1	2	−1	−1	2	−1	−1	−2	1	1

Table 3. Coefficients of symmetry coordinates for coupling vibrations in the $(MCl_4)_4$ model.

Species of T_d	(Species of C_{3v})	Norm. factor	Coefficients of											
			$\tau_1{}^A$	$\tau_2{}^A$	$\tau_3{}^A$	$\tau_1{}^B$	$\tau_2{}^B$	$\tau_3{}^B$	$\tau_1{}^C$	$\tau_2{}^C$	$\tau_3{}^C$	$\tau_1{}^D$	$\tau_2{}^D$	$\tau_3{}^D$
A_2	(a_2)	$12^{-1/2}$	1	1	1	1	1	1	1	1	1	1	1	1
$E;\,a$	(e)	$8^{-1/2}$	0	−1	1	0	−1	1	0	−1	1	0	−1	1
$E;\,b$	(e)	$24^{-1/2}$	2	−1	−1	2	−1	−1	2	−1	−1	2	−1	−1
$F_1;\,a$	(a_2)	$6^{-1/2}$	0	0	0	1	1	1	−1	−1	−1	0	0	0
$F_1;\,b$	(a_2)	$6^{-1/2}$	−1	−1	−1	0	0	0	0	0	0	1	1	1
$F_1;\,c$	(a_2)	$8^{-1/2}$	1	1	1	−1	−1	−1	−1	−1	−1	1	1	1
$F_1;\,a$	(e)	$48^{-1/2}$	0	−3	3	−2	1	1	2	−1	−1	0	3	−3
$F_1;\,b$	(e)	$48^{-1/2}$	2	−1	−1	0	3	−3	0	−3	3	−2	1	1
$F_1;\,c$	(e)	$24^{-1/2}$	2	−1	−1	−2	1	1	−2	1	1	2	−1	−1
$F_2;\,a$	(e)	1/4	0	−1	1	2	−1	−1	−2	1	1	0	1	−1
$F_2;\,b$	(e)	1/4	2	−1	−1	0	−1	1	0	1	−1	−2	1	1
$F_2;\,c$	(e)	$8^{-1/2}$	0	1	−1	0	−1	1	0	−1	1	0	1	−1

the couplings. These tables have general applicability for symmetry coordinates of tetrahedral complexes with trigonal ligands. Hence they are useful supplements to the theory [21, 23].

Numerical Computations and Discussions for $(TeCl_4)_4$ and $(SeCl_4)_4$

Structural Parameters

An idealized structure with right angles in the ligand parts as well as the cube was adopted. The interatomic distances

$$\text{Te–Cl}_b = 2.93\ \text{Å}, \quad \text{Te–Cl}_t = 2.32\ \text{Å}$$

for $(TeCl_4)_4$ were taken from Buss et al. [13]. The corresponding distances for $(SeCl_4)_4$ were estimated to

$$\text{Se–Cl}_b = 2.69\ \text{Å}, \quad \text{Se–Cl}_t = 2.13\ \text{Å}$$

from the analogy with $(TeCl_4)_4$ and a suggestion for the Se–Cl_t bond from Gerding et al. [18].

Initial Force Field

A very simple force field approximation was chosen in order to calculate a set of initial vibrational frequencies. It is represented by a diagonal force-constant matrix in terms of the valence coordinates including redundancies. When using same values for some of the different bending force constants the number of adjustable parameters was reduced to four. For $(TeCl_4)_4$ the following numerical values were found, after several trials, to give frequencies with reasonable magnitudes.

$$f_r(\text{Te–Cl}_b) = 1.5\ \text{mdyne/Å},$$
$$f_d(\text{Te–Cl}_t) = 2.15\ \text{mdyne/Å},$$
$$f_\gamma = f_\beta = 0.2\ \text{mdyne/Å},$$
$$f_\alpha = f_\delta = 0.1\ \text{mdyne/Å}.$$

The value for f_d is sufficiently comparable with the reported stretching force constant in $TeCl_3^+$, viz. 2.27 mdyne/Å [27]. For $(SeCl_4)_4$ the following stretching force constants were adopted for the initial force field.

$$f_r(\text{Se–Cl}_b) = 1.3\ \text{mdyne/Å},$$
$$f_d(\text{Se–Cl}_t) = 1.9\ \text{mdyne/Å}.$$

The values of bending force constants were all transferred from $(TeCl_4)_4$; see above. For $SeCl_3^+$ a value of 2.26 mdyne/Å for the stretching force constant is reported [27].

The approximate calculated frequencies from the initial force fields for $(TeCl_4)_4$ and $(SeCl_4)_4$ are shown in Tables 4 and 5, respectively.

Assignment of Vibrational Frequencies

The initial calculated frequencies were used as an aid in assignments of experimental frequencies from literature.

For $(TeCl_4)_4$ the tentatively assigned experimental frequencies are found in Table 4. The numerical values are taken from Ponsioen et al. [20], and specifically Raman data in species A_1 and E (which are infrared inactive) and infrared data in species F_2 (which is both Raman and infrared active). The 148 cm^{-1} band was accepted among the F_2 fundamentals although it is supposed to be overlapped by a water band in infrared [20]. This assignment is supported by the observation of 150 cm^{-1} in Raman [19, 20]. The strongest Raman bands should preferably be assigned as A_1 frequencies. Hence our assignment of the Raman-active frequencies was guided by the two cited reports [18, 19]. According to Gerding et al. [18] the strongest Raman bands (in cm^{-1}) are 374, 342, 191 and 143 in accord with our assignment (cf. Table 4). Two

Table 4. Calculated vibrational frequencies (cm^{-1}) for $(TeCl_4)_4$.

Species	Initial	Final	PED[a]
A_1	387	374[b]	$69\,d + 30\,r$
	345	349[b]	$40\,\alpha + 40\,r + 23\,d$
	194	192[b]	$93\,\gamma + 36\,\alpha$
	126	137[b]	$35\,\alpha + 30\,r$
A_2	95	95	$100\,\tau$
E	382	360[b]	$87\,d + 22\,r$
	309	338[b]	$67\,r$
	180	203[b]	$147\,\gamma + 130\,\tau$
	153	186[b]	$63\,\gamma$
	48	48	$188\,\alpha + 124\,\tau$
F_1	390	390	$68\,d + 32\,r$
	311	311	$71\,r + 28\,d$
	180	180	$168\,\gamma + 150\,\tau'$
	134	134	$28\,\gamma + 24\,\tau'$
	92	92	$83\,\tau$
F_2	408	374[b]	$97\,\alpha + 94\,r + 52\,d'$
	393	363[b]	$64\,d + 48\,r' + 26\,r$
	331	343[b]	$93\,\alpha + 59\,r + 32\,\tau + 29\,r' + 21\,d$
	321	335[b]	$47\,\alpha + 37\,r' + 35\,d' + 33\,r$
	193	192[b]	$98\,\gamma$
	169	168[b]	$225\,\gamma' + 87\,\tau + 22\,\alpha$
	122	148[b]	$81\,\alpha$
	84	84	$100\,\tau + 52\,r$

[a] Potential energy distribution terms $100\,F_{ii}\,L_{ik}^2/\lambda_k$; terms below 20 are omitted.

[b] Adjusted to observed frequencies [20].

Table 5. Calculated vibrational frequencies ($\mathrm{cm^{-1}}$) for $(\mathrm{SeCl_4})_4$.

Species	Initial	Final	PED[a]
A_1	405	388[b]	$69\,d + 24\,r$
	333	344[b]	$43\,\alpha + 39\,r$
	205	206[b]	$69\,\gamma + 35\,\alpha$
	131	127[b]	$35\,r + 28\,\alpha + 25\,\gamma$
A_2	95	95	$100\,\tau$
E	400	371[b]	$83\,d + 27\,r$
	292	338[b]	$59\,r$
	191	219[b]	$91\,\tau + 67\,\gamma$
	157	162[b]	$118\,\gamma + 21\,\tau$
	50	50	$161\,\alpha + 116\,\tau$
F_1	410	410	$61\,d + 36\,r$
	294	294	$68\,r + 31\,d$
	185	185	$160\,\tau' + 146\,\gamma$
	140	140	$48\,\gamma$
	92	92	$81\,\tau$
F_2	432	393	$87\,r + 82\,\alpha + 45\,d'$
	412	375[b]	$62\,d + 48\,r' + 25\,r$
	316	350[b]	$80\,\alpha + 47\,r + 31\,\tau + 27\,r'$
	304	276[b]	$62\,\alpha + 45\,d' + 43\,r' + 42\,r$
	200	192[b]	$92\,\gamma$
	171	168[b]	$213\,\gamma' + 77\,\tau + 32\,\alpha$
	132	148[b]	$76\,\alpha$
	86	86	$90\,\tau + 52\,r$

[a,b] See footnotes to Table 4.

of these bands obviously correspond to 375 vs and 347 s reported by Demiray [19]. She has reported two additional strong Raman bands, viz. 80 s and 55 s, which according to our analysis nicely can be assigned as the lowest F_2 and E frequency, respectively.

For $(\mathrm{SeCl_4})_4$ the tentative assignment of frequencies is found in Table 5. Basically the same principles were used as for the $(\mathrm{TeCl_4})_4$ assignment described above. The Raman bands of Gerding et al. [18] for the Se compound are not so distinct as in the case of Te. They have reported (in $\mathrm{cm^{-1}}$) 388, 346, 206 and 96 as the most prominent bands. We find strong evidence from the analogy between the two compounds and our calculation that 127 $\mathrm{cm^{-1}}$, also observed by Gerding et al. [18], should be assigned as the lowest A_1 fundamental. The infrared spectrum of $(\mathrm{SeCl_4})_4$ is of considerably less quality than that of $(\mathrm{TeCl_4})_4$ [20].

Final Force Field

The initial force fields for $(\mathrm{TeCl_4})_4$ and $(\mathrm{SeCl_4})_4$ were adjusted to fit exactly the observed frequencies according to our assignments described above. For the unobserved frequencies the values were transferred from the results of our initial calculations (cf. Tables 4 and 5) with one exception; for the highest F_2 frequency of $(\mathrm{SeCl_4})_4$ the value of 393 $\mathrm{cm^{-1}}$ was adopted rather than 432 $\mathrm{cm^{-1}}$. The modified value was produced by an auxiliary calculation, where the F_2 symmetry force constants were changed in a way guided by the shifts from the initial to the final force constants in $(\mathrm{TeCl_4})_4$; see below.

The symmetry force constants consistent with the complete sets of final frequencies for $(\mathrm{TeCl_4})_4$ (see Table 4) and $(\mathrm{SeCl_4})_4$ (see Table 5) are shown in Tables 6 and 7, respectively.

Potential Energy Distribution

The final force fields were used to calculate the potential energy distribution [28] in terms of the symmetry coordinates. The results are shown in Tables 4 and 5. For the sake of convenience the symmetry coordinates are identified by means of the appropriate types of valence coordinates; cf. Table 1.

Mean Amplitudes of Vibration

The final force fields were used to calculate the mean amplitudes of vibration [29] for all types of bonded and nonbonded interatomic distances for the molecules here considered. The results at the temperatures of absolute zero and 298 K for $(\mathrm{TeCl_4})_4$ and $(\mathrm{SeCl_4})_4$ are given in Tables 8 and 9, respectively. The interatomic separations calculated from the adopted structural parameters for the equilibrium structure are included (in parentheses) in order to facilitate the identification of the fifteen types of distances.

Numerical Computations for $\mathrm{TeCl_4}$

Frequency Shifts from Tetramer to Monomer

The frequency shifts of tetramerization of $\mathrm{TeCl_4}$ were studied in the following way. A hypothetical idealized C_{2v} model for the $\mathrm{TeCl_4}$ molecule was assumed with a linear axial part and right-angled equatorial part. All Te-Cl distances were taken to be 2.32 Å as the Te-$\mathrm{Cl_t}$ distance in $(\mathrm{TeCl_4})_4$. Also the force constant of 2.15 mdyne/Å for all these bonds was transferred from the tetrameric model and taken as equal to $f(\mathrm{Te{-}Cl_t})$ of the initial force field. For all the five (nonlinear) bending force constants the value of 0.2 mdyne/Å was adopted.

The calculated approximate frequencies with the two-parameter force field described above are shown

Table 6. Final symmetry force constants (mdyne/Å) for $(TeCl_4)_4$.

Species A_1	2.07					Species A_2	
	−0.00	0.31				0.15	
	0.09	−0.04	1.58				
	0.00	−0.10	0.04	0.28			
Species E	2.06						
	0.04	0.82					
	0.23	0.09	1.77				
	−0.05	−0.46	−0.04	0.58			
	−0.08	−0.57	−0.06	0.48	0.78		
Species F_1	2.15						
	0.00	0.58					
	0.00	−0.30	1.93				
	0.00	0.00	0.00	0.15			
	0.00	−0.41	0.33	0.00	0.60		
Species F_2							
2.03							
−0.00	0.30						
−0.00	−0.00	2.10					
0.01	−0.03	0.06	0.65				
−0.08	0.19	−0.33	−0.81	4.55			
−0.03	0.14	−0.10	−0.61	2.14	1.61		
−0.20	0.06	0.16	0.56	−1.33	−0.95	2.70	
−0.03	0.03	−0.09	−0.50	0.88	0.67	−0.60	0.69

Table 7. Final symmetry force constants (mdyne/Å) for $(SeCl_4)_4$.

Species A_1	1.81					Species A_2	
	0.03	0.29				0.15	
	0.07	0.01	1.29				
	−0.01	−0.07	−0.03	0.26			
Species E	1.86						
	−0.02	0.63					
	0.26	−0.06	1.57				
	−0.03	−0.35	0.08	0.52			
	−0.08	−0.46	0.05	0.42	0.71		
Species F_1	1.90						
	0.00	0.58					
	0.00	−0.30	1.73				
	0.00	0.00	0.00	0.15			
	0.00	−0.41	0.33	0.00	0.60		
Species F_2							
1.76							
−0.00	0.28						
0.13	−0.02	1.67					
0.01	−0.02	0.02	0.61				
−0.14	0.20	−0.15	−0.66	3.81			
0.01	0.13	−0.04	−0.52	1.80	1.40		
−0.17	0.06	−0.11	0.50	−1.03	−0.88	2.34	
−0.04	0.02	−0.05	−0.45	0.69	0.55	−0.51	0.63

in Table 10 in correlation with the initial, approximate $(TeCl_4)_4$ frequencies. In this correlation only the numerical coincidences were taken into account. In this table also the activities in Raman and infrared are indicated. As a whole it is predicted that the monomer should give rise to 9 Raman active and 8 infrared active frequencies, while the numbers are 17 and 8, respectively, in the case of the tetramer. It is interesting that the number of infrared active frequencies does not change on tetramerization, and they are also predicted to be roughly within the same orders of magnitude. The

Table 8. Mean amplitudes of vibration (Å) for $(TeCl_4)_4$.

Distance type	(Equil. dist./Å)	Mean amplitude $T = 0$	298 K
Te-Cl_b	(2.93)	0.0424	0.0531
Te-Cl_t	(2.32)	0.0412	0.0496
Te ... Te	(4.14)	0.0389	0.0721
Te ... Cl_b	(5.07)	0.0483	0.0718
Cl_b ... Cl_b	(4.14)	0.0554	0.0769
Te ... Cl_t	(4.75)	0.068	0.144
Te ... Cl_t	(6.01)	0.055	0.095
Cl_b ... Cl_t	(3.74)	0.066	0.109
Cl_b ... Cl_t	(5.25)	0.054	0.069
Cl_b ... Cl_t	(6.69)	0.065	0.108
Cl_t ... Cl_t	(3.28)	0.066	0.099
Cl_t ... Cl_t	(4.14)	0.098	0.229
Cl_t ... Cl_t	(6.44)	0.083	0.174
Cl_t ... Cl_t	(7.42)	0.076	0.140
Cl_t ... Cl_t	(8.12)	0.064	0.103

Table 9. Mean amplitudes of vibration (Å) for $(SeCl_4)_4$.

Distance type	(Equil. dist./Å)	Mean amplitude $T = 0$	298 K
Se-Cl_b	(2.69)	0.0451	0.0570
Se-Cl_t	(2.13)	0.0440	0.0536
Se ... Se	(3.80)	0.0447	0.0766
Se ... Cl_b	(4.66)	0.0517	0.0759
Cl_b ... Cl_b	(3.80)	0.0556	0.0767
Se ... Cl_t	(4.36)	0.071	0.146
Se ... Cl_t	(5.52)	0.059	0.100
Cl_b ... Cl_t	(3.43)	0.068	0.112
Cl_b ... Cl_t	(4.82)	0.057	0.074
Cl_b ... Cl_t	(6.14)	0.067	0.112
Cl_t ... Cl_t	(3.01)	0.067	0.102
Cl_t ... Cl_t	(3.80)	0.099	0.232
Cl_t ... Cl_t	(5.92)	0.085	0.176
Cl_t ... Cl_t	(6.82)	0.078	0.145
Cl_t ... Cl_t	(7.45)	0.067	0.108

Raman spectrum on the other hand, is expected to change drastically from the monomer to the tetramer.

Normal Coordinate Analysis for Gaseous $TeCl_4$

It is of interest to report the more realistic computations for $TeCl_4$(g), using the observed structural parameters from electron diffraction [11]. Table 11 shows the frequency shifts when passing from the hypothetical (idealized) structure to the realistic one and maintaining the approximate force constants (see above). It should be noticed that some of these shifts are not at all negligible.

A final assignment of the vibrational frequencies was produced with the aid of experimental data from Beattie et al. [30]; cf. Table 11. A final force field in exact consistence with this assignment was deduced, but is not specified here for the sake of brevity.

Mean Amplitudes of Vibration

In the early (1940) gas electron diffraction work on $TeCl_4$ no mean amplitudes of vibration were reported. In a modern re-investigation this part of the work could hardly be neglected. Furthermore a set of calculated mean amplitudes from spectro-

Table 10. Calculated approximate vibrational frequencies (cm^{-1}) for $TeCl_4$ tetramer and monomer[a].

$(TeCl_4)_4$ — T_d[b]					$TeCl_4$ — C_{2v}[c]			
A_1	A_2	E	F_1	F_2	a_1	a_2	b_1	b_2
Ra	ia	Ra	ia	Ra IR	Ra IR	Ra	Ra IR	Ra IR
				408			406	
			390	393				
387		382			367			364
345				331				
				321	321			
		309	311					
194				193				
		180	180				186	
				169		169		
		153			156			
			134					
126				122				117
	95		92		110			
		48		84				

[a] Ra = Raman active, IR = infrared active, ia = inactive.
[b] Species designations in capital letters.
[c] Species designations in small letters.

Table 11. Calculated vibrational frequencies (cm^{-1}) for $TeCl_4$.

Species	Approximate[a] (i)	(ii)	Final
a_1	367	355	382[b]
	321	321	290[b]
	156	158	158[b]
	110	96	72[b]
a_2	169	177	177
b_1	406	406	314[b]
	186	180	180
b_2	364	377	382[b]
	117	133	133

[a] (i) hypothetical (idealized) structure; (ii) realistic structure for $TeCl_4$ (g).

[b] Observed [30].

Table 12. Mean amplitudes of vibration (Å) for $TeCl_4$.

Distance type[a]	(Equil. dist./Å)	Mean amplitude $T = 0$	298 K
Te-Cl_{ax}	(2.330)	0.0447	0.0567
Te-Cl_{eq}	(2.330)	0.0400	0.0472
$Cl_{ax} \ldots Cl_{ax}$	(4.642)	0.0581	0.0783
$Cl_{eq} \ldots Cl_{eq}$	(3.726)	0.0661	0.1023
$Cl_{ax} \ldots Cl_{eq}$	(3.380)	0.0711	0.1208

[a] ax = axial; eq = equatorial.

scopic data would be very useful in the interpretation of electron diffraction data. Hence we give here such values (Table 12), calculated for the first time. They were obtained from the force field adjusted to the final assignment of vibrational frequencies shown in Table 11.

Acknowledgement

Financial support to BNC from The Norwegian Research Council for Science and the Humanities is gratefully acknowledged.

[1] V. C. Ewing and L. E. Sutton, Trans. Faraday Soc. **59**, 1241 (1963).
[2] K. Kimura and S. H. Bauer, J. Chem. Phys. **39**, 3172 (1963).
[3] G. W. Chantry and V. C. Ewing, Mol. Phys. **5**, 209 (1962).
[4] M. G. Krishna Pillai, K. Ramaswamy, and R. Pichai, Austral. J. Chem. **18**, 1575 (1965).
[5] K. Venkateswarlu and S. Mariam, Indian J. Pure Appl. Phys. **3**, 472 (1965).
[6] I. W. Levin and Ch. V. Berney, J. Chem. Phys. **44**, 2557 (1966).
[7] S. J. Cyvin, Acta Chem. Scand. **23**, 576 (1969).
[8] K. O. Christe and W. Sawodny, J. Chem. Phys. **52**, 6320 (1970).
[9] K. O. Christe, W. Sawodny, and P. Pulay, J. Mol. Struct. **21**, 158 (1974).
[10] K. O. Christe, E. C. Curtis, C. J. Schack, S. J. Cyvin, J. Brunvoll, and W. Sawodny, Spectrochim. Acta **32 A**, 1141 (1976).
[11] D. P. Stevenson and V. Schomaker, J. Am. Chem. Soc. **62**, 1267 (1940).
[12] H. J. M. Bowen, Nature **172**, 171 (1953).
[13] B. Buss and B. Krebs, Angew. Chem. **82**, 446 (1970).
[14] B. Buss and B. Krebs, Inorg. Chem. **10**, 2795 (1971).
[15] A. W. Cordes, R. F. Kruh, E. K. Gordon, and M. K. Kemp, Acta Cryst. **17**, 756 (1964).
[16] C. B. Schoemaker and S. C. Abrahams, Acta Cryst. **18**, 296 (1965).
[17] T. Okuda, K. Yamada, Y. Furukawa, and H. Negita, Bull. Chem. Soc. Japan **48**, 392 (1975).
[18] H. Gerding and H. Houtgraf, Rec. Trav. Chim. **73**, 737 (1954).
[19] A. F. Demiray, Dissertation, Technische Universität Clausthal 1977.
[20] R. Ponsioen and D. J. Stufkens, Rec. Trav. Chim. **90**, 521 (1971).
[21] S. J. Cyvin and L. Lyhamn, J. Mol. Struct. **25**, 151 (1975).
[22] R. Andreassen, S. J. Cyvin, and L. Lyhamn, J. Mol. Struct. **25**, 155 (1975).
[23] S. J. Cyvin, J. Mol. Struct. **30**, 311 (1976).
[24] S. J. Cyvin, B. N. Cyvin, R. Andreassen, and A. Müller, J. Mol. Struct. **25**, 141 (1975).
[25] J. C. Whitmer and S. J. Cyvin, J. Mol. Struct. **38**, 277 (1977).
[26] L. Lyhamn, S. J. Cyvin, B. N. Cyvin, and J. Brunvoll, Z. Naturforsch. **31 a**, 1589 (1976).
[27] H. Siebert, Anwendungen der Schwingungsspektroskopie in der anorganischen Chemie, Springer-Verlag, Berlin 1966.
[28] K. Nakamoto, Infrared Spectra of Inorganic and Coordination Compounds, Wiley, New York 1963; Second Edition 1970.
[29] S. J. Cyvin, Molecular Vibrations and Mean Square Amplitudes, Universitetsforlaget, Oslo, and Elsevier, Amsterdam 1968.
[30] J. R. Beattie, O. Bizri, H. E. Blayden, S. B. Brumbach, A. Bukovszky, T. R. Gilson, R. Moss, and B. A. Phillips, J. Chem. Soc. Dalton **16**, 1747 (1974).